2007

Formation of In- (2×1) and in Islands on Si (100) - (2×1) by Femtosecond Pulsed Laser Deposition

M. A. Hafez
Old Dominion University

H. E. Elsayed-Ali
Old Dominion University, helsayed@odu.edu

Formation of In-(2×1) and In islands on Si(100)-(2×1) by femtosecond pulsed laser deposition

M. A. Hafez and H. E. Elsayed-Ali[a)]
*Department of Electrical and Computer Engineering, Old Dominion University, Norfolk, Virginia 23529
and Applied Research Center, Old Dominion Unversity, Norfolk, Virginia 23529*

The growth of indium on a vicinal Si(100)-(2×1) surface at room temperature by femtosecond pulsed laser deposition (fsPLD) was investigated by *in situ* reflection high-energy electron diffraction (RHEED). Recovery of the RHEED intensity was observed between laser pulses and when the growth was terminated. The surface diffusion coefficient of deposited In on initial two-dimensional (2D) In-(2×1) layer was determined. As growth proceeds, three-dimensional In islands grew on the 2D In-(2×1) layer. The RHEED specular profile was analyzed during film growth, while the grown In islands were examined by *ex situ* atomic force microscopy. The full width at half maximum of the specular peak decreased during the deposition, indicative of well-ordered growth and an increase of the island size. The In islands developed into elongated-polyhedral, circular, and triangular shapes. The elongated and triangular islands were highly oriented, parallel and perpendicular to the surface terrace edges, while the circular islands show a top flat surface. Deposition of In on Si(100)-(2×1) by fsPLD influenced the formation of the initial In-(2×1) layer and the morphology of the grown islands. © *2007 American Institute of Physics*. [DOI: 10.1063/1.2738388]

I. INTRODUCTION

Growth of group-III metals on Si surfaces has been the subject of many theoretical and experimental studies due to its fundamental and technological interests. Many studies have focused on structure determination and behavior of group-III induced reconstructions on Si surfaces.[1–5] It has been observed that group-III metals grown on Si form self-assembled nanowires and nanoclusters with potential applications in devices.[6–8] Moreover, understanding the growth of group-III metals is important in metallization applications and in the growth of III-V and III-IV semiconductors on Si.[9,10] The study of the initial growth modes of group-III metals on Si surfaces and the subsequent film morphology development is important for further developments in electronic and optoelectronic devices.

Indium was previously grown on Si(100)-(2×1) using molecular beam epitaxy (MBE) and conventional evaporation.[11–15] In these studies, the growth was observed by low-energy electron diffraction (LEED), scanning tunneling microscopy (STM), reflection high-energy electron diffraction (RHEED), time-of-flight impact collision ion scattering spectroscopy (TOF-ICISS), and Auger electron spectroscopy (AES). Results showed that the In-(2×2) was the main structure observed in the initial growth of In on Si(100)-(2×1) below 150 °C. STM studies showed that Al, Ga, and In initially form long one-dimensional ad-dimers on the Si(100)-(2×1) surface.[3,5] This growth mode continued until the (2×2) structure was completed at 0.5 ML (monolayer) [1 ML=6.8×10^14 atoms/cm^2 for unreconstructed Si(100) surface].[2,16,17] Other submonolayer phases of Al and

In deposited on a wide terrace single domain Si(100)-(2×1) were also observed using LEED.[4] For surfaces annealed at ∼100 °C following deposition at room temperature (RT), sequences of (2×3) and (2×5) LEED patterns at ∼0.3 and ∼0.4 ML, respectively, were observed before forming the In-(2×2) reconstruction.[4]

Compared with surface microscopy techniques, surface electron diffraction, such as RHEED, probes a large area (e.g., 1 mm^2). Thus, diffraction provides information on the structure and morphology averaged over the probed area and can provide quantitative information on average values, which can be used to study growth kinetics.[18] During deposition, RHEED provides real time information on nucleation and monolayer formation. For example, the growth transition from layer-by-layer to step flow mode on vicinal surfaces has been used to estimate diffusion parameters from RHEED observations.[19,20] The recovery of the RHEED intensity after interruption of MBE growth has been used to study the film growth kinetics.[21–27]

Pulsed laser deposition (PLD) has been shown to provide a high nucleation density of deposits and improve two-dimensional (2D) growth, which led to growth of high quality metallic thin films.[28] PLD produces highly energetic species with high instantaneous deposition rates, which have the potential to assist in crystalline phase formation in thin films.[29] These characteristic features of PLD can alter the thin film properties. A theoretical study of growth for Ag/Ag(111) indicated that increasing the incident atom energy, from 0.1 to 10 eV, changed the growth from three-dimensional (3D) to layer-by-layer growth, through enhanced diffusion of surface atoms from unstable positions to stable positions.[30] In a molecular dynamics simulation, an incident energetic Si atomic beam on Si(100) and Si(111)

a)Electronic mail: helsayed@odu.edu

surfaces induced local surface heating and formed a crystal-line film, at less than half the absolute temperature required for thermal adatoms.[31]

We have studied the growth mode and morphology of In on Si(100)-(2×1) for femtosecond pulsed laser deposition (fsPLD).[32] Indium grew by formation of a 2D In-(2×1) layer followed by 3D islands. The present work focuses on the growth kinetics of the initial 2D In-(2×1) layer and extends the study of the grown film morphology. The diffusion parameters of deposited In on surface terraces were investigated by quantitative RHEED. The intensity and full width at half maximum (FWHM) of the RHEED specular beam were measured during In growth. The grown film morphology was examined by *ex situ* atomic force microscopy (AFM) and STM. The formation of the initial In-(2×1) structure and the In island morphology were related to the growth kinetics by fsPLD.

II. EXPERIMENT

The growth was performed in an ultrahigh-vacuum (UHV) PLD system. The base pressure during deposition was in the low 10^{-9} Torr range. An amplified Ti:sapphire laser, (pulse width ∼130 fs FWHM) operating at a wavelength of 800 nm and repetition rates of 1 and 2 Hz, was used to ablate the In target. The laser was incident on a 99.99% pure In target at ∼45° and focused on the In target using a convex lens with a 30 cm focal length. The target was rotated at a speed of 2 rpm to minimize particulate formation. The target-to-substrate distance was fixed at ∼5 cm. RHEED was used to observe the surface structure of the substrate and the film growth during deposition. The RHEED electron gun was operated at electron energy of 8.6 keV. The diffraction patterns were acquired by a charge-coupled device (CCD) camera. Real time evaluation of the intensity and FWHM of the RHEED beams were performed and correlated with the deposition conditions. RHEED analyses along and across the diffracted beams were obtained in the reciprocal space and then converted to length scales after taking into account the instrumental response. The uncertainties in the electron energy and the RHEED camera length were determined by measuring the in-plane lattice parameter of the Si(100) surface. The morphology of the grown films was imaged and characterized *ex situ* with a noncontact AFM and STM.

The ∼5×10 mm^2 Si substrates were cut from a Si(100) wafer (*p* type, boron doped, 500 μm thick). The Si surfaces were misoriented from the low-index (100) plane by 1.0° toward the ⟨110⟩±0.5°. The Si(100)-(2×1) surface was prepared by chemical etching just prior to being loaded into the UHV chamber. This was followed by *in situ* heat cleaning to 600 °C for several hours using direct current, then flash heating at ∼1100 °C to remove native oxides and carbon. Following surface cleaning, short streaks in the RHEED zeroth Laue semicircle and Kikushi lines were visible. Just prior to In deposition, the Si(100)-(2×1) was raised in temperature to ∼1000 °C for ∼2 min by direct-current heating. The heating was then terminated and the substrate cooled down to RT. RHEED patterns acquired after annealing
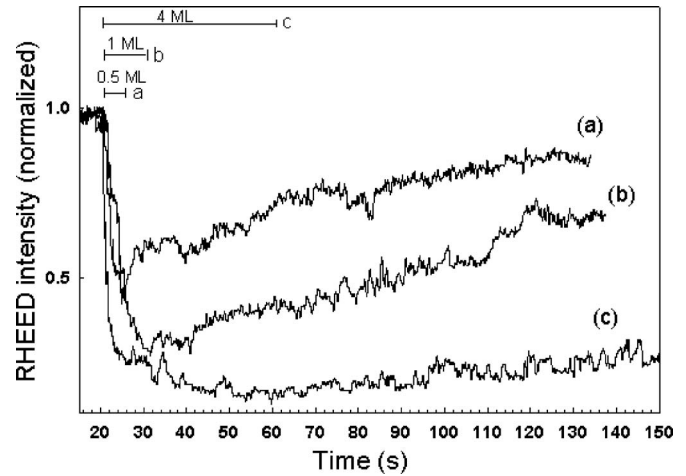

FIG. 1. Specular beam RHEED intensity after deposition of (a) ∼0.5 ML on an initial ∼1.5 ML In-(2×1), (b) an additional ∼1 ML giving a total coverage of ∼3 ML, and (c) ∼4 ML on an initial ∼5 ML of In. The deposition was performed with the laser operated at 2 Hz laser repetition rate and 0.5 J/cm^2 laser fluence. The RHEED electron beam was incident along the [011] azimuth down the vicinal Si surface. The initial 2D layer formed in the In-(2×1) structure.

showed clean reconstructed Si(100)-(2×1) with less RHEED background, indicating a smooth well-ordered surface. PLD of In on Si(100)-(2×1) reported here focuses on growth with the Si substrate kept at RT.

Calibration of the deposition rate per laser pulse was accomplished using RHEED oscillations, which provides a highly accurate method to obtain film thickness. Since RHEED oscillations were observed only at substrate temperatures near the melting point of In, we performed several depositions at conditions that allowed RHEED oscillations to be observed. The deposition rate was estimated to be ∼0.05 ML/pulse. This was confirmed by a postdeposition estimate of film thickness using a profilometer.

III. RESULTS AND DISCUSSION

A. RHEED intensity recovery and growth kinetics

RHEED intensity recovery was used to investigate growth kinetics of deposition of In on Si(100)-(2×1). The In films were prepared on the Si(100)-(2×1) at RT by fsPLD, while the RHEED specular beam intensity was measured at the Bragg condition as a function of In deposition thickness. The growth was performed using interval deposition, i.e., deposition by a number of laser pulses with a given amount of In, followed by an interval of no deposition, with this sequence then repeated. The laser was operated at a 2 Hz repetition rate and an energy density of 0.5 J/cm^2 on the In target. During the deposition of the initial ∼1.5 ML, the (2×1) structure was preserved, as observed from the RHEED patterns. The RHEED electron beam was incident along the [011] azimuth down the vicinal Si surface. At other azimuthal directions, such as [013] and [0$\bar{1}\bar{1}$], the RHEED patterns showed no change in the predeposition Si(100)-(2×1) pattern, although there was an observed change of the in-plane lattice spacing as discussed later. Figure 1 shows specular beam intensities taken from a series of sequential In
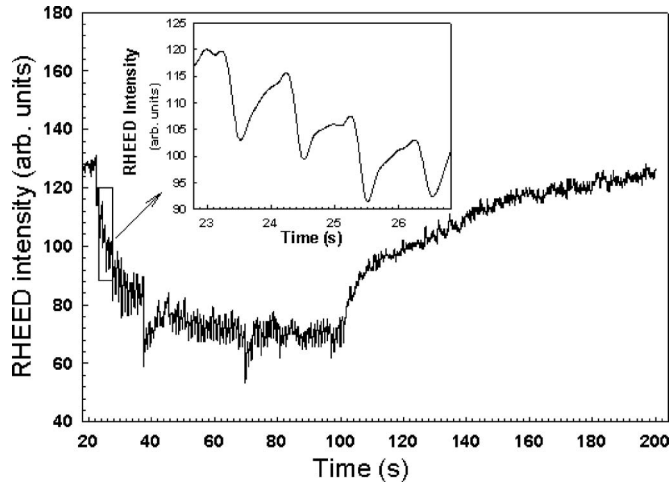
FIG. 2. RHEED intensity of the (20) diffraction beam as a function of In deposition time on Si(100)-(2×1) at a substrate temperature of ~145 °C. The laser was operated at 1 Hz repetition rate with an energy density of 0.5 J/cm^2 on the In target. Relaxation of the RHEED intensity was observed during In deposition after each laser pulse as seen in the inset figure, which displays the RHEED intensity for laser pulse numbers 2–5 from starting the deposition. The laser was turned on at 21 s and turned off at 100 s.

depositions on top of the initial 1.5 ML that had the In-(2×1) structure. Recovery of the RHEED specular intensity is monitored after growth termination by turning off the laser upon deposition of a known In thickness. After terminating the deposition at ~0.5 ML of In (total In coverage ~2 ML), the specular beam intensity increased to a value close to its predeposition intensity, as shown in Fig. 1(a). This indicates that the deposited In diffused on surface terraces and grew epitaxially, thus, resulting in increased long-range order to a value close to that prior to deposition. After deposition of the next 1 ML giving a total coverage of ~3 ML of In, the recovery of the RHEED specular intensity became slower, as shown in Fig. 1(b). The RHEED intensity recovery is dependent on the smoothness of the surface before deposition, the deposited In diffusion energy, and the amount of the deposited In. Deposition of ~4 ML of In on a substrate already covered by 5 ML In led to a continuous decrease in the specular intensity with only weak RHEED intensity recovery after deposition, as shown in Fig. 1(c). This indicates an increase of surface roughness due to island nucleation on the surface. The RHEED intensity recovery after growth termination is observed up to an In coverage of ~7 ML and was accompanied by maintaining the In-(2×1) structure.

Deposition of In on Si(100)-(2×1) at substrate temperatures near but below the In bulk melting point showed recovery of the RHEED specular beam intensity after growth termination. Figure 2 shows the RHEED intensity of the (20) diffracted beam for a substrate temperature of ~145 °C. The laser was operated at 1 Hz repetition rate with an energy density of 0.5 J/cm^2 on the In target. The growth was performed on ~2.7 ML of In that was initially prepared on Si(100)-(2×1). When the growth was started, a reduction in the RHEED intensity was observed. After growth termination, the RHEED intensity recovered its original value within a certain time. The recovery of the RHEED beam intensity after growth termination is known to be characteristic of step

flow growth.[19,33] In a previous STM study of In on Si(100) at RT, it was found that a flat 2D In-(2×1) island of ~1.4 ML, on the initial In-(2×2) layer, grew preferentially at the surface terrace edges.[34] In the step flow growth mode, the deposited material attaches to the step terrace edges and the surface recovers the original surface order, along with the RHEED intensity. Step flow growth in PLD was previously observed and showed relaxation of RHEED intensity after each laser pulse.[35,36] For a substrate temperature of ~145 °C, relaxation of the RHEED intensity was observed after each laser pulse during fsPLD of In, as shown in the inset of Fig. 2. To capture this relaxation of the RHEED intensity, the CCD camera was operated at a fast frame rate. The intensity of the ($\bar{2}$0) diffracted beam showed similar relaxation behavior during the fsPLD of In but out of phase to the (20) diffracted beam. This RHEED relaxation indicates that surface smoothing occurred between deposition pulses. The recovery and relaxation of the RHEED intensity, as shown in Fig. 2, are attributed to step flow growth of the 2D In-(2×1) layer.

The characteristic diffusion parameters of deposited In on the In-(2×1) wetting layers can be measured from the recovery time profile of the RHEED specular beam intensity. The diffusion length ℓ is related to the diffusion coefficient D by $\ell = (2D\tau)^{1/2}$, where τ is the average diffusion time on the surface terraces, which depends on the density of nucleation sites and the diffusion velocity.[19] Figure 3(a) shows the RHEED recovery of the specular beam intensity of Fig. 1(a) after growth termination. The RHEED intensity exhibited a rapid, then slow recovery, indicating that the growth kinetics varied during the entire surface recovery. Lewis *et al.* and Joyce *et al.* have shown that surface recovery after growth termination occurs in two stages, a fast and a slow process.[25,37] The RHEED intensity in Fig. 3(a) is well represented by a sum of two exponentials in the form of $I(t) = A_0 + A_1[1 - \exp(-t/\tau_1)] + A_2[1 - \exp(-t/\tau_2)]$, where A_0, A_1, and A_2 are constants, while τ_1 and τ_2 represent the time constants which correspond to the fast and slow processes of recovery. From a curve fit to the RHEED intensity, the time constants for recovery are obtained such that $\tau_1 = 2 \pm 0.4$ s, while $\tau_2 = 80 \pm 5$ s.

For film growth by step flow mode, one can use the intensities of the specular beam or higher-order diffraction beams in RHEED to monitor the diffusion process.[38] Figure 3(b) shows a curve fit to the intensity recovery of the (20) beam in Fig. 2 after growth termination. In this case, the time constants τ_1 and τ_2 are found to be 1.9 ± 0.3 and 53 ± 2 s, respectively. The inset of Fig. 3(b) shows RHEED intensity behavior between the second and third deposition laser pulses from starting the deposition. The RHEED intensity dropped and then increased before the next pulse. Each laser pulse ablates the In target, creating ~3.4×10^{13} atoms/cm^2 of In to the surface. In this case, the RHEED intensity decreased because of the increased random distribution of incoming In deposits on the surface. The deposited In reorganized by diffusion on the surface, increasing the RHEED intensity until the arrival of the next In flux. During In deposition, the surface smoothness changed with each laser pulse in a periodic fashion, which can be viewed as a kind of
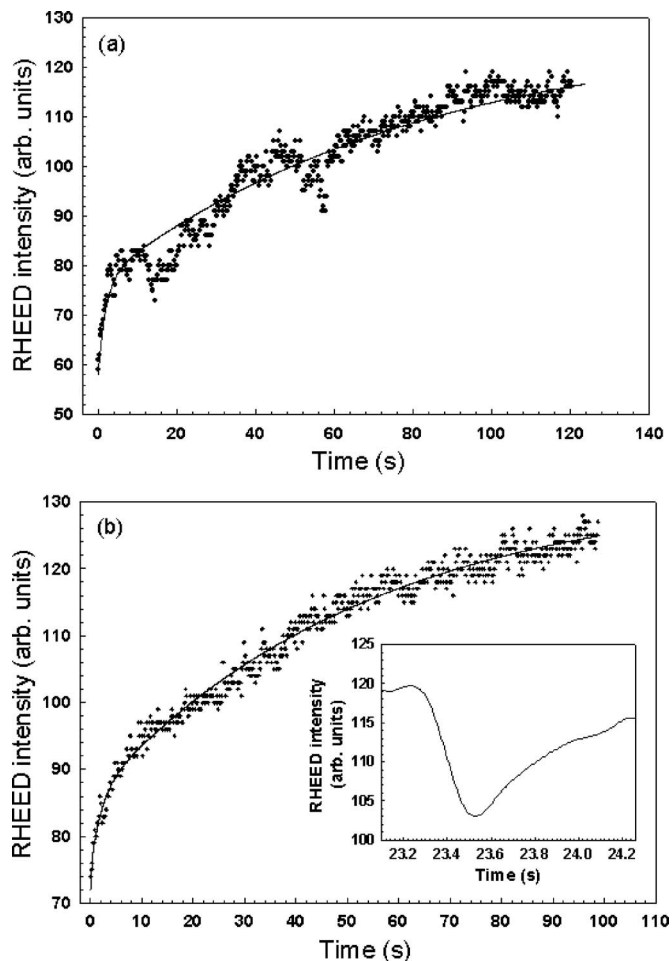
FIG. 3. (a) Recovery of the RHEED specular beam intensity after deposition of In at RT and coverage of ~2 ML. (b) Recovery of the RHEED (20) beam intensity after deposition of In at a substrate temperature of ~145 °C performed on initially ~2.7 ML of In. The RHEED intensity shows initial fast increase and then a slow recovery, characterized by two exponential recovery times τ_1 and τ_2, respectively. The x axis starts with 0 in (a) and (b) for curve fitting. The inset in (b) shows a decrease and then a relaxation of the RHEED intensity between the second and third deposition laser pulses.
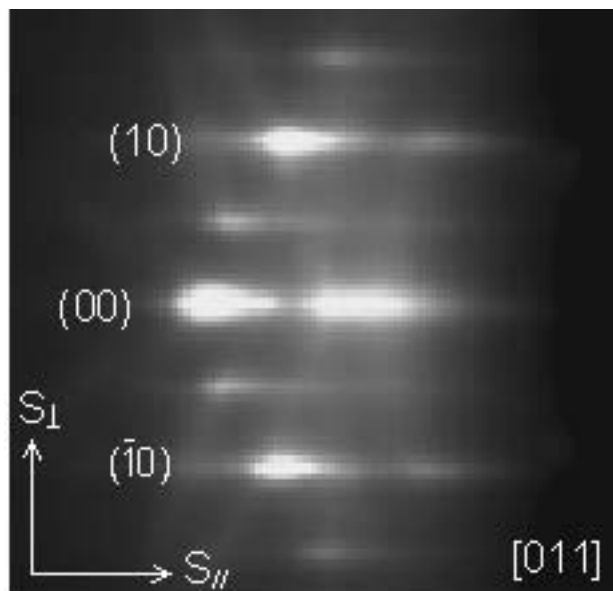

FIG. 4. RHEED pattern of the Si(100)-(2×1) surface taken at the out-of-phase condition corresponding to θ_{inc} of ~65 mrad. The primary electron energy of 8.6 keV was incident down the staircase of the vicinal surface along the [011] azimuth. $S_\parallel$ and $S_\perp$ are the components of the momentum transfer parallel and perpendicular to the electron beam, respectively. The specular beam is split in the $S_\parallel$ direction into two peaks around a central part, which is located within the RHEED zeroth Laue zone.

interrupted growth. The relaxation time depends on the substrate temperature, surface condition, deposited material, and the repetition rate of the laser pulse.[39] Upon growth termination the surface order recovered to its original state as before deposition. The RHEED intensity showed fast and slow recoveries after growth termination with each recovery rate characterized by its diffusion coefficient. For films grown by step flow, diffusion to the terrace step edges with a time constant τ depends on the surface terrace width. Therefore, knowing the surface terrace width, one can determine the surface diffusion coefficient D.

The average terrace width of the vicinal Si(100)-(2×1) surface is expected to be affected by the chemical etching and heat cleaning. Thus, the average terrace width of the Si(100)-(2×1) substrate was measured before In deposition. This was accomplished by directing the RHEED electron beam down the staircase of the vicinal Si surface, along the [011] azimuth. The specular beam showed splitting peaks at the out-of-phase condition defined by $2d \sin \theta_{inc} = (n+1/2)\lambda$, where d is the monolayer step height, θ_{inc} is the incident

angle corresponding to the out-of-phase condition, n is an integer, and λ is the electron wavelength. The out-of-phase diffraction condition was used to study clean vicinal surface structures.[40,41] Figure 4 shows RHEED pattern of the vicinal Si(100)-(2×1) showing splitting of the specular beam in the $S_\parallel$ direction, where $S_\parallel$ and $S_\perp$ are the components of the momentum transfer parallel and perpendicular to the electron beam, respectively. The out-of-phase angle of incidence θ_{inc} was ~65 mrad. The average terrace width was determined from the split peak spacing $L = 2\pi/(d\theta)k \sin \theta_{inc}$, where $k = 47.78$ Å^{-1} is the Ewald sphere radius and $d\theta = 32.7$ mrad is the splitting angle. Taking into account the RHEED instrumental response of 0.20 ± 0.02 Å^{-1}, the average terrace width of the Si(100)-(2×1) surface was obtained to be $L = 61 \pm 10$ Å. The instrumental response was obtained from the FWHM along the specular beam at the Bragg diffraction condition. The corresponding misorientation angle for the vicinal Si(100)-(2×1) substrate with a step height of 1.36 Å is approximately 1.3°.

The surface diffusion coefficient D of the fast and slow recovery processes of deposited In over the In-(2×1) wetting layer grown by fsPLD was determined. In the case of film growth by the step flow mode, the diffusion length ℓ is limited by the terrace width and thus is equal to L. By knowing the diffusion parameters τ and ℓ, D can be determined. From the RHEED intensity recovery of Fig. 3(a), the In diffusion coefficient at RT is found to be $D_1 = 9 \pm 1.6 \times 10^{-14}$ cm^2/s for the initial fast recovery and $D_2 = 2 \pm 0.4 \times 10^{-15}$ cm^2/s for the slow recovery. The In diffusion coefficient of the RHEED intensity recovery, Fig. 3(b), for the deposition conditions at substrate temperature of ~145 °C is $D_1 = 9 \pm 1.5 \times 10^{-14}$ cm^2/s for the initial fast recovery and $D_2 = 3 \pm 0.6 \times 10^{-15}$ cm^2/s for the slow recovery. The experi-

mental errors in calculating D arise from the instrumental response and uncertainty in determining the split peak spacing.

The surface processes that lead to the recovery of the RHEED intensity depend on the growth mode and the deposition parameters. In MBE growth of GaAs, the initial recovery was attributed to surface reconstruction changes and the slow process of rearrangement of 2D islands.[37] Neave *et al.* have explained the initial recovery in the growth of GaAs(001)-(2×4) by Ga–As bond dissociation at step edges.[24] Indium incorporation during the growth of Si(100) has shown a strong surface segregation leading to formation of an abrupt interface with Si.[11,42] Deposition by MBE is characterized by a steady-state, thermal atom flux, while in PLD, pulsed plumes of energetic species are obtained. Indium atoms landing on the Si substrate with a high deposition rate lead to the formation of small In clusters. The drop of the specular RHEED intensity after each fsPLD pulse, shown in the inset of Fig. 2, indicates the reduction of surface order after the plume arrives on the surface. At the terrace step edges, atoms have lower coordination, making them more reactive. Because of their high reactivity, surface step edges provide preferred sites for film growth. Metal islands and clusters were observed to decorate the steps of the substrates.[34,43,44] The growth of the 2D In-(2×1) layer occurred by surface diffusion to the step edges, which was responsible for the observed RHEED intensity recovery. In a proposed model for growth of superconducting thin films by PLD, the RHEED intensity recovery was attributed to the diffusion of material units, with D of the order of 10^{-12} cm^2/s, rather than to the diffusion of adatoms.[45] In our case, the initial fast RHEED recovery is expected to be due to surface diffusion of In clusters, with D of the order of 10^{-14} cm^2/s. These In clusters diffused toward terrace edges, in a step flow growth mode, thereby causing an increase in the RHEED intensity. Previous experimental observation of fast diffusion of clusters and a study of 2D island diffusion on surfaces were reported.[46–48] Diffusion of adatom and vacancy islands of Ag on Ag(100) was found to occur by different diffusion mechanisms.[49,50] The slower process following the initial fast decay in the RHEED intensity was attributed to recovery of long-range order of the terrace step edges.

B. Island growth and morphology

We next discuss the development of In film morphology on Si(100)-(2×1) in fsPLD. Figure 5 shows the RHEED specular beam intensity of In on Si(100)-(2×1) grown at RT using a laser pulse repetition rate of 2 Hz and a laser energy density of 0.5 J/cm^2. The electron beam was incident with θ_{inc} of ~68 mrad along the [011] azimuth. RHEED patterns of the Si(100)-(2×1) substrate and the grown In film are shown in the inset of Fig. 5. The RHEED intensity of the specular beam as well as higher-order diffracted beams decreased after starting the In growth. Formation of the In-(2×1) wetting layer on the Si surface is associated with the initial drop of the intensity. The RHEED specular intensity then decreased slowly, indicating development of surface
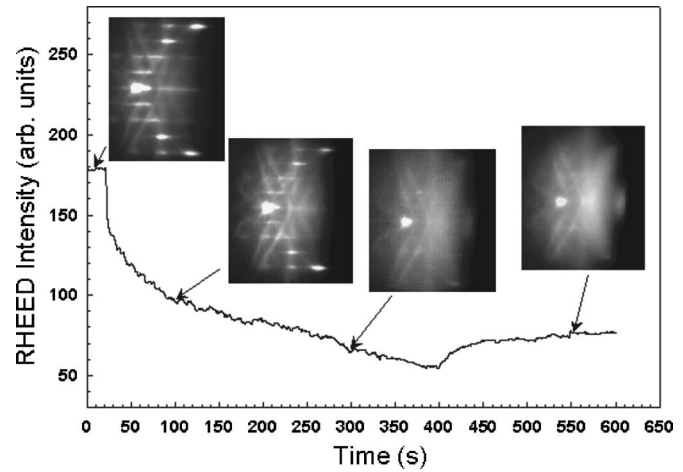

FIG. 5. RHEED intensity of the specular beam was monitored with deposition time. The electron beam was incident with θ_{inc} of ~68 mrad along the [011] substrate azimuth. The deposition conditions were 2 Hz laser repetition rate and 0.5 J/cm^2 laser energy density. RHEED patterns taken in the [011] azimuth of the Si(100)-(2×1) substrate and of the grown In film at 100 s, 296 s, and postdeposition are shown in the inset. The In-(2×1) structure was preserved during the initial growth. The laser was turned on at 20 s and turned off at 400 s.

roughness due to growth of In islands in the Stranski-Krastanov (SK) mode. This result is consistent with the previously reported MBE growth of In on Si(100)-(2×1), where transmission diffraction spots were not observed in the RHEED patterns because of the combination of the low coverage area and small density of islands.[11] Postdeposition RHEED pattern of ~38 ML of In on Si(100)-(2×1), shown in the inset of Fig. 5, has wide faint rings on a high background, indicating random in-plane crystallographic orientation of the grown 3D islands.

The peak profile of the RHEED intensity is analyzed during the growth of the In thin film by measuring the FWHM across the specular beam ($S_{\perp}$ direction). The FWHM is measured close to the in-phase diffraction condition down the vicinal Si surface during deposition. As the islands grow on the surface, their size distribution can be determined from the intensity profile. The size distribution is extracted from a Gaussian profile fit to the RHEED specular spot. An example of this curve fit is shown in Fig. 6(a) for film coverages of ~7 and ~14 ML, giving FWHMs of 0.39 and 0.35 Å^{-1}, respectively. The width of the specular beam profile in Fig. 6(a) is a convolution of instrumental broadening and broadening in the reciprocal lattice rods of the grown In domains on the surface. The instrumental response was determined from the FWHM of the main electron beam on the RHEED screen and is found to be 0.30 ± 0.015 Å^{-1} in the $S_{\perp}$ direction. Taking into account the instrumental response, Fig. 6(b) shows the change in the FWHM of the specular beam intensity profile with deposition time corresponding to film coverage between ~0.3 and ~14 ML (left y axis). The FWHM decreased from ~0.22 to 0.04 Å^{-1}, which indicates an increase in the average surface coherence.[51] Figure 6(b) (right y axis) shows the specular spot intensity-to-background ratio I_{spec}/I_{back} during film deposition, where I_{spec} and I_{back} are the specular peak and RHEED background intensities, respectively. The background intensity I_{back} is measured at a loca-
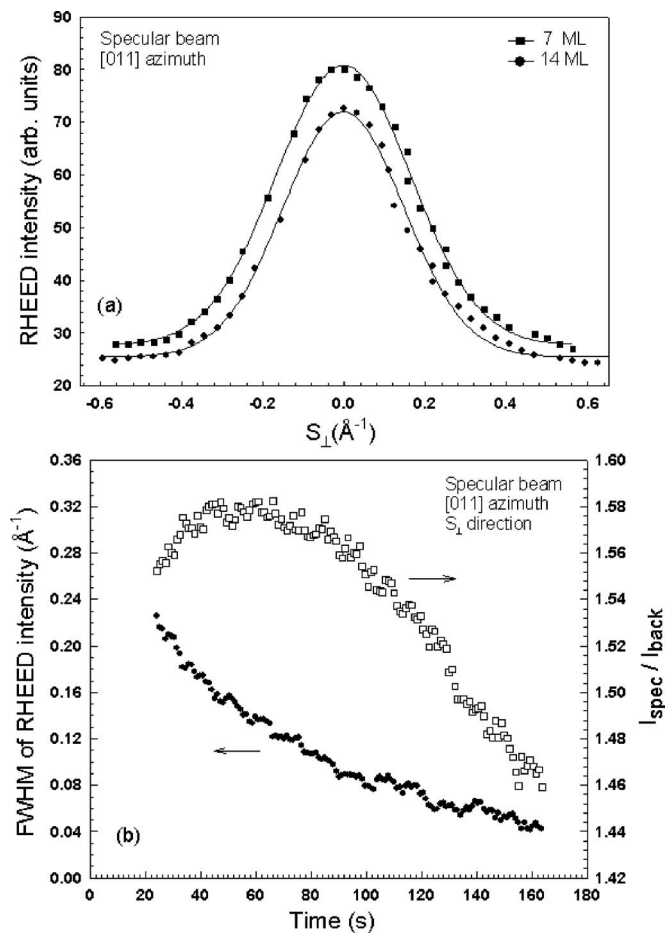
FIG. 6. (a) RHEED intensity profiles of the specular beam at film coverages of ~7 and ~14 ML vs the momentum transfer $S_\perp$ parallel to the substrate surface. (b) FWHM of specular RHEED intensity profile as a function of the deposition time taking into account an instrumental response of 0.30 ± 0.015 Å^{-1} in the $S_\perp$ direction. The FWHM decreased from ~0.22 to 0.04 Å^{-1}. The spot intensity-to-background ratio of I_{spec}/I_{back} (open squares) during film deposition is shown, where I_{spec} and I_{back} are the specular peak and RHEED background intensities, respectively.
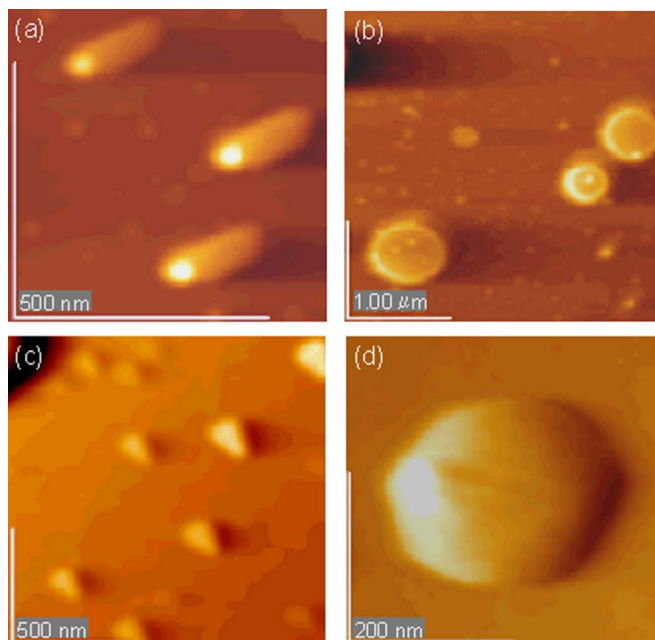

FIG. 7. (Color online) AFM images taken after deposition of In on Si(100)-(2×1) substrate at RT by fsPLD (corresponding to the postdeposition RHEED pattern in Fig. 5). The 3D islands in (a)–(c) show elongated, circular, and triangular shapes, respectively. The elongated and triangular islands are highly oriented toward [011] and [01$\bar{1}$] azimuths of the Si(100)-(2×1) surface. (d) Hexagonal-shaped In island.

tion between the specular and (10) diffracted beams. Its value is dependent on step edge density and roughness of the grown film. The ratio I_{spec}/I_{back} increased initially during growth of the 2D wetting layer, indicating an improvement of the surface quality. Then, it started to decrease with In thickness after ~7 ML. The film coverage at which the transition from 2D growth to 3D growth occurs depends on the difference between the In and Si crystal structures as well as on the structure of the initial In-(2×1) layer. During the transition growth stage, small In islands grew on the surface before completion of the underlying layers. As growth proceeds, the size of the islands increased, leading to shadowing of the incident electron beam, which yields low specular beam intensity.

Next, the morphology of the grown In film was examined *ex situ* using AFM. Figure 7 shows AFM images of the grown crystalline In islands on the Si(100)-(2×1) substrate at RT, which correspond to the postdeposition RHEED pattern in Fig. 5. The In islands took a variety of elongated, circular, and triangular shapes as shown in Figs. 7(a)–7(c), respectively. These 3D islands grew on a smooth 2D In sur-

face as seen in the AFM images. This is consistent with the RHEED observation of SK growth. The elongated and triangular islands show preferential growth orientations toward the [011] and [01$\bar{1}$] azimuths of the Si(100)-(2×1) surface. These orientations were confirmed by taking AFM images of a Si(100) surface, without deposition of In film, and the AFM tip was scanned over the same direction similar to that examined for samples after In deposition. The directions [011] and [01$\bar{1}$] were determined by observing the orientation of terrace edges of the vicinal surface. These growth directions are affected by the 2D In layer on the Si vicinal surface, where the (2×1) domains are known to be rotated by 90° alternately parallel and normal to the step edges of terraces.[52] We also observed hexagonal-shaped faceted In islands as shown in Fig. 7(d).

Three-dimensional AFM images of the elongated In islands show polyhedral shapes, for which an example is shown in Fig. 8(a). Line profiles taken along and across the polyhedral island imaged in Fig. 8(a) show a major axis of ~215 nm along the [011] direction and a width of ~100 nm, as shown in Figs. 8(b) and 8(c). The top plane of the island in Fig. 8(b) is inclined to the substrate surface by an angle of $\theta = 3° \pm 0.6°$, while the front plane made an angle $\theta = 15° \pm 0.8°$ with the substrate surface. The sidewall planes in Fig. 8(c) made an angle $\theta = 25° \pm 3.3°$ with the substrate surface. Some of the grown elongated islands did not show a faceted polyhedral structure. Figure 9(a) is a 3D image of a circular island, which shows that its perimeter has a higher edge forming a ring around an inner flat central part, which is parallel to the Si(100) surface. On top of the island, some growth features are observed. Figure 9(b) is a line profile
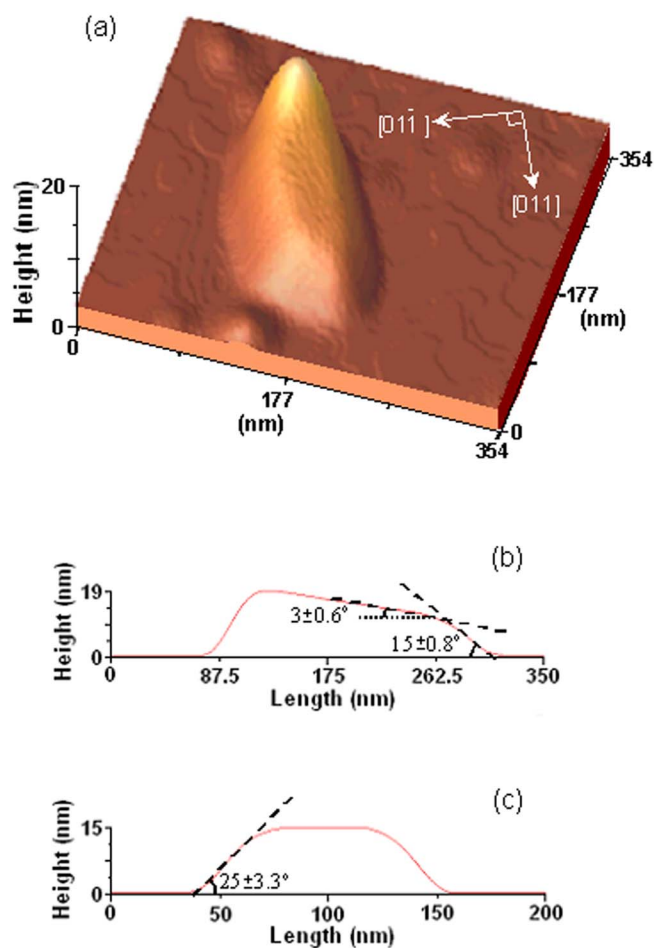
FIG. 8. (Color online) (a) 3D AFM image of an elongated In island oriented toward the [011] substrate azimuth. (b) and (c) are line profiles taken along and across the elongated island in (a), respectively.
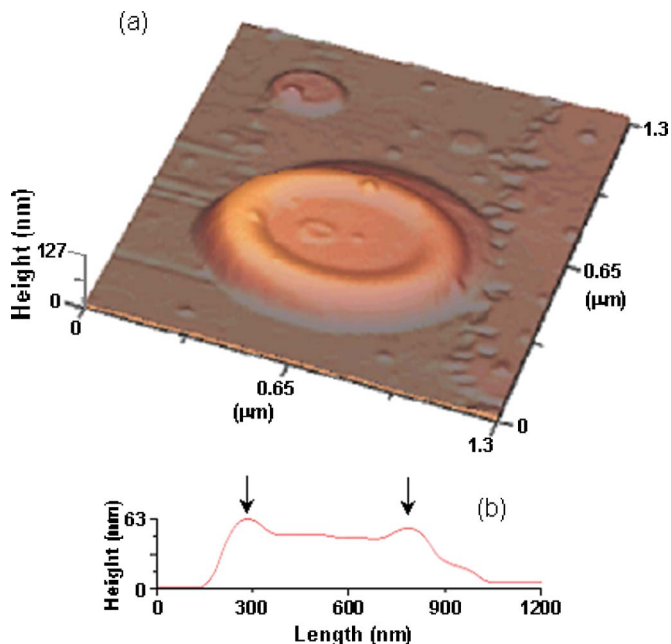

FIG. 9. (Color online) (a) 3D AFM image of a circular In island. (b) Line profile across the center of the island in (a) showing a higher edge surrounding a flat central part as indicated by arrows.

taken across the island in Fig. 9(a), showing that the rounded edge has a height of ~60 nm while the flat top plane has a height of ~52 nm. Figure 10(a) is a 3D STM image of another In circular island, showing complex ring structure with nanoscale roughness on the ring and top surface of the island. Figure 10(b) is a 3D STM image taken in the region between the large circular islands, showing small In islands of different sizes. The elongated-polyhedral and circular islands were found with a low number density but had mostly large size and regular well-defined step edges.

The AFM and STM observation shows that the height-to-diameter aspect ratios of the circular islands are small. For islands with a mean diameter of 220 nm, the heights measured from the rounded edges are around 6% of the diameter. For islands of a diameter in the range of 490–690 nm, the average height is 11% of the diameter. The circular islands show central flat top planes, which covered ~40% of the total island surface area. In a previous study of growth of In on GaAs(001) by MBE, In islands with flat top surfaces were observed after using Sb as a surfactant.[53] For elongated islands, the height-to-length aspect ratios are relatively small. The measured heights were in the range of 2%–7% of the elongated axes length. The small height-to-length aspect ratios of In islands and the decrease of the FWHM of the

specular RHEED beam with In coverage, shown in Fig. 6(b), suggest that In nucleation took place at the edges of the islands more than on their top surface.

C. fsPLD effects

At the initial stages of In growth on the Si(100)-(2×1) at RT by fsPLD, the (2×1) RHEED pattern was preserved but was accompanied by a sudden drop in the RHEED intensity of the specular beam as well as the higher-order diffracted beams. Moreover, a decrease in the in-plane lattice spacing of the grown film occurred. We did not observe development of another RHEED pattern such as (2×2) during the In deposition. Using STM, Zhu et al.[54] reported that In-(2×2) and In-(2×1) reconstructions coexist at coverages between 0.5 and 1.0 ML, while in a STM observation Ryu et al.[15] did not observe In-(2×1) reconstruction. In MBE growth of In/Si(100)−(2×1), the In-(2×2) structure was observed by RHEED and LEED.[11] In general, thin film structure and morphology depend on the deposition conditions such as the incident atom energy, deposition rate, and coverage. The In-(2×1) structure has not been previously reported as an initial layer in the deposition of In on Si(100)-(2×1).

Femtosecond PLD is known to result in the formation of a plume containing energetic species.[55] The high energy of atoms and ions in the ablated In plume affects the In film growth in two ways. The first is due to the impact of the incident energetic In species with the Si substrate, leading to displacement in substrate surface lattice sites and possible removal of the Si(100)-(2×1) reconstruction. The second effect is due to the large deposited In diffusion rate because of its high kinetic energy and local surface lattice heating due to inelastic energy transfer from different In plume species. Northrup et al.[56] used first-principles total-energy calcula-
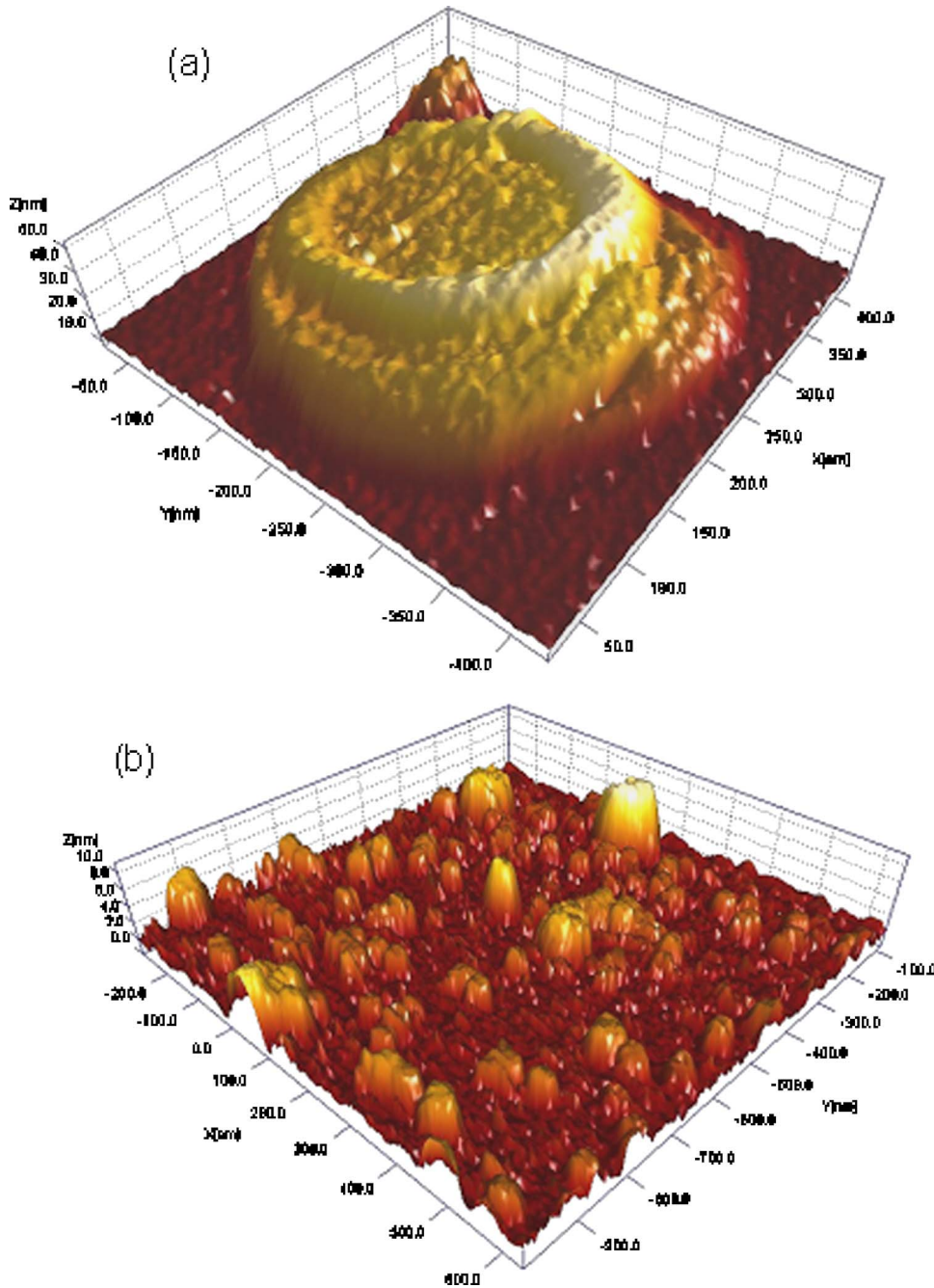
FIG. 10. (Color online) STM 3D scans of (a) an In circular island and (b) small In islands.

tions to show that the In-(2×1) dimer structure occurs rather than In-(2×2) only when the In adsorbate chemical potential is larger than that of the In bulk under nonequilibrium conditions. The In-(2×1) structure considered has a 1 ML of In dimers and is obtained by replacing the Si dimers on Si(100)-(2×1) with In dimers. Accordingly, the In-(2×1) structure would not occur under equilibrium conditions. However, the high kinetic energy of In atoms and ions in fsPLD could allow for nonequilibrium conditions to occur. In addition, the incident energetic In species in fsPLD can affect island morphology which depends on the surface diffusion of the deposited In.

The (2×1) reconstruction induced by group-III atoms on the Si(100) surface cannot be explained by the dimer-on-dimer model.[57] Therefore, in the In/Si(100) system, the underlayer Si(100)-(2×1) reconstruction is most likely re-moved and the top surface layer becomes bulklike terminated: Si(100)-(1×1) structure with two dangling bonds per Si atom. The deposited In atoms occupy the dangling bonds of the Si surface. To achieve the threefold coordination configuration, each In atom bonds to one In atom from the first layer and two Si atoms from the second layer in order to reduce the number of unsaturated bonds at the surface. Therefore, a coverage of 1 ML of In is needed to saturate all the dangling bonds of the underlying Si(100)-(1×1) surface, whereas in the case of the In-(2×2) structure, a coverage of 0.5 ML saturates the dimerized Si(100)-(2×1) surface. We used the RHEED patterns of the In film to estimate the in-plane lattice parameter a. This parameter is measured from the separation of the first-order RHEED peaks, fitted to Gaussian line shapes, which are taken in the [011] azimuthal direction of the Si surface. The

in-plane lattice parameter is found to be $a = 3.65 \pm 0.1$ Å, while the surface lattice parameters of In(100) and Si(100) are 3.24 and 3.84 Å, respectively. This indicates that the first In monolayers formed a strained 2D layer, creating a (2×1) RHEED structure similar to Si(100)-(2×1) but with a different lattice parameter a.

Further In growth by fsPLD on the initial strained In-(2×1) layer showed formation of different island morphologies. The 3D island morphology is affected by kinetics and the structure of the In-(2×1) layer. In PLD, the expanding plume containing different species has a wide range of energy.[58] When the In deposits were influenced by the dimer structure of the initial In-(2×1) layer, elongated-polyhedral islands developed, which exhibit preferential growth orientation with respect to the Si substrate. This type of island was observed in MBE growth of In on Si(100)-(2×1) surface and was referred to as anisotropic growth due to the anisotropic strain in the (2×1) structure.[11] When the In deposits have enough diffusion energy to overcome the anisotropic strain in the underlying In-(2×1) first layers, the deposits move across as well as along the dimer rows and the growth results in the formation of different island morphologies such as the circular and triangular shapes. Quantitative analysis of the FWHM of the RHEED specular beam, parallel to the substrate surface, indicated an increase of the long-range order of the In islands with deposition time. The grown In island shapes and their lateral size-to-height ratios indicated that growth of islands spreads laterally, more than vertically, due to preferential diffusion of In to the islands' edges. This can be seen in the elongation and flattened top surface of the grown polyhedral and circular In islands, respectively.

IV. CONCLUSION

The fsPLD of In on vicinal Si(100)-(2×1) influenced the formation of the initial In-(2×1) layer and the island morphology. On the 2D In-(2×1) layer, surface order recovery was observed during deposition and after growth termination. The surface diffusion coefficient of deposited In was measured by quantitative RHEED. The 3D In islands grew into polyhedral-elongated, circular, and triangular shapes. The occurrence of theses 3D In island morphology indicates that the growth was caused to undergo the influence of the structure of the 2D In-(2×1) layer and In diffusion. The results suggest that fsPLD of In removed the reconstruction of the Si(100)-(2×1) surface in the early growth and formed the initial In-(2×1) layer.

[1]A. A. Baski, J. Nogami, and C. F. Quate, Phys. Rev. B **43**, 9316 (1991).
[2]J. Nogami, A. A. Baski, and C. F. Quate, Phys. Rev. B **44**, 1415 (1991).
[3]H. Itoh, J. Itoh, A. Schmid, and T. Ichinokawa, Phys. Rev. B **48**, 14663 (1993).
[4]H. W. Yeom, T. Abukawa, M. Nakamura, S. Suzuki, S. Sato, K. Sakamoto, T. Sakamoto, and S. Kono, Surf. Sci. **341**, 328 (1995).
[5]N. Takeuchi, Phys. Rev. B **63**, 035311 (2001).
[6]D. J.-L. Li, X.-L. Liang, J.-F. Jia, X. Liu, J.-Z. Wang, E.-G. Wang, and Q.-K. Xue, Appl. Phys. Lett. **79**, 2826 (2001).
[7]J.-Z. Wang, J.-F. Jia, X. Liu, W.-D. Chen, and Q.-K. Xue, Phys. Rev. B **65**, 235303 (2002).
[8]J.-L. Li *et al.*, Phys. Rev. Lett. **88**, 066101 (2002).
[9]P. C. Sharma, K. W. Alt, D. Y. Yeh, and K. L. Wang, Appl. Phys. Lett. **75**, 1273 (1999).
[10]B. H. Koo, T. Hanada, H. Makino, J. H. Chang, and T. Yao, J. Cryst. Growth **229**, 142 (2001).
[11]J. Knall, J. Sundgren, G. Hansson, and J. E. Greene, Surf. Sci. **166**, 512 (1986).
[12]M. M. R. Evans, J. C. Glueckstein, and J. Nogami, Surf. Sci. **406**, 246 (1998).
[13]J.-T. Ryu, K. Kui, K. Noda, M. Katayama, and K. Oura, Surf. Sci. **401**, L425 (1998).
[14]M. M. R. Evans and J. Nogami, Phys. Rev. B **59**, 7644 (1999).
[15]J. T. Ryu, O. Kubo, H. Tani, T. Harada, M. Katayama, and K. Oura, Surf. Sci. **433–435**, 575 (1999).
[16]A. A. Baski, J. Nogami, and C. F. Quate, J. Vac. Sci. Technol. A **8**, 245 (1990).
[17]A. A. Baski, J. Nogami, and C. F. Quate, J. Vac. Sci. Technol. A **9**, 1946 (1991).
[18]H. Busch and M. Henzler, Phys. Rev. B **41**, 4891 (1990).
[19]J. H. Neave, P. J. Dobson, B. A. Joyce, and J. Zhang, Appl. Phys. Lett. **47**, 100 (1985).
[20]N. Bertru, M. Nouaoura, J. Bonnet, and L. Lassabatere, J. Cryst. Growth **160**, 1 (1996).
[21]D. D. Vvedensky and S. Clarke, Surf. Sci. **225**, 373 (1990).
[22]H. Sakaki, M. Tanaka, and J. Yoshino, Jpn. J. Appl. Phys., Part 1 **24**, 1417 (1985).
[23]A. Madhukar, T. C. Lee, M. U. Yen, P. Chen, J. Y. Kim, S. V. Ghaisas, and P. G. Newman, Appl. Phys. Lett. **46**, 1148 (1985).
[24]J. H. Neave, B. A. Joyce, P. J. Dobson, and N. Norton, Appl. Phys. A: Solids Surf. **31**, 1 (1983).
[25]B. F. Lewis, F. J. Grunthaner, A. Madhukar, T. C. Lee, and R. Fernandez, J. Vac. Sci. Technol. B **3**, 1317 (1985).
[26]S. Clarke, D. D. Vvedensky, and M. W. Ricketts, J. Cryst. Growth **95**, 28 (1989).
[27]S. V. Ghaisas and A. Madhukar, J. Appl. Phys. **65**, 3872 (1989).
[28]J. Shen, Z. Gai, and J. Kirschner, Surf. Sci. Rep. **52**, 163 (2004).
[29]J. C. Miller and R. F. Haglund, *Laser Ablation and Desorption*, Experimental Methods in the Physical Sciences Vol. 30 (Academic, Boston, 1998).
[30]C. M. Gilmore and J. A. Sprague, Phys. Rev. B **44**, 8950 (1991).
[31]G. H. Gilmer and C. Roland, Appl. Phys. Lett. **65**, 824 (1994).
[32]M. A. Hafez, M. S. Hegazy, and H. E. Elsayed-Ali, J. Vac. Sci. Technol. A **23**, 1681 (2005).
[33]T. Frey, C. C. Chi, C. C. Tsuei, T. Shaw, and F. Bozso, Phys. Rev. B **49**, 3483 (1994).
[34]O. Kubo, J. T. Ryu, H. Tani, T. Harada, M. Katayama, and K. Oura, Jpn. J. Appl. Phys., Part 1 **38**, 3849 (1999).
[35]M. Lippmaa, N. Nakagawa, M. Kawasaki, S. Ohashi, Y. Inaguma, M. Itoh, and H. Koinuma, Appl. Phys. Lett. **74**, 3543 (1999).
[36]J. Choi, C. B. Eom, G. Rijnders, H. Rogalla, and D. H. A. Blank, Appl. Phys. Lett. **79**, 1447 (2001).
[37]B. A. Joyce, T. Shitara, A. Yoshinaga, D. D. Vvedensky, J. H. Neave, and J. Zhang, Appl. Surf. Sci. **60/61**, 200 (1992).
[38]X. D. Zhu, Phys. Rev. B **57**, 9478 (1998).
[39]D. H. A. Blank, G. J. H. M. Rijnders, G. Koster, and H. Rogalla, Appl. Surf. Sci. **138–139**, 17 (1999).
[40]Z. H. Zhang, B. Lin, X. L. Zeng, and H. E. Elsayed-Ali, Phys. Rev. B **57**, 9262 (1998).
[41]M. A. Hafez and H. E. Elsayed-Ali, J. Appl. Phys. **91**, 1256 (2002).
[42]J. Knall, J.-E. Sundgren, J. E. Greene, A. Rockett, and S. A. Barnett, Appl. Phys. Lett. **45**, 689 (1984).
[43]J. A. Venables, Thin Solid Films **50**, 357 (1978).
[44]G. M. Francis, L. Kuipers, J. R. A. Cleaver, and R. E. Palmer, J. Appl. Phys. **79**, 2942 (1996).
[45]V. S. Achutharaman, N. Chandrasekhar, O. T. Valls, and A. M. Goldman, Phys. Rev. B **50**, 8122 (1994).
[46]L. Bardotti, P. Jensen, A. Hoareau, M. Treilleux, and B. Cabaud, Phys. Rev. Lett. **74**, 4694 (1995).
[47]P. Deltour, J.-L. Barrat, and P. Jensen, Phys. Rev. Lett. **78**, 4597 (1997).

[48]A. Bogicevic, S. Liu, J. Jacobsen, B. Lundqvist, and H. Metiu, Phys. Rev. B **57**, 9459 (1998).

[49]J.-M. Wen, S.-L. Chang, J. W. Burnett, J. W. Evans, and P. A. Thiel, Phys. Rev. Lett. **73**, 2591 (1994).

[50]J.-M. Wen, J. W. Evans, M. C. Bartelt, J. W. Burnett, and P. A. Thiel, Phys. Rev. Lett. **76**, 652 (1996).

[51]J. M. Van Hove, P. Pukite, and P. I. Cohen, J. Vac. Sci. Technol. A **1**, 609 (1983).

[52]K. Oura, V. G. Lifshits, A. A. Saranin, A. V. Zotov, and M. Katayama, *Surface Science* (Springer-Verlag, Berlin, 2003).

[53]S. Schintke, U. Resch-Esser, N. Esser, A. Krost, W. Richter, and B. O. Fimland, Surf. Sci. **377–379**, 953 (1997).

[54]C. Zhu, T. Hayashi, S. Misawa, and S. Tsukahara, Jpn. J. Appl. Phys., Part 1 **33**, 3706 (1994).

[55]J. Perrier, E. Millon, W. Seiler, C. Boulmer-Leborgne, V. Carcin, O. Albert, J. C. Loulergue, and J. Etchepare, J. Appl. Phys. **91**, 690 (2002).

[56]J. E. Northrup, M. C. Schabel, C. J. Karlsson, and R. I. Uhrberg, Phys. Rev. B **44**, 13799 (1991).

[57]W. Monch, *Semiconductor Surfaces and Interfaces* (Springer-Verlag, Berlin, 1993).

[58]D. B. Chrisey and G. K. Hubler, *Pulsed Laser Deposition of Thin Films* (Wiley, New York, 1994).